PROCEEDINGS A

rspa.royalsocietypublishing.org

Research

Cite this article: Zhao J, Jia Y, Wei N, Rabczuk T. 2015 Binding energy and mechanical stability of two parallel and crossing carbon nanotubes. *Proc. R. Soc. A* **471**: 20150229. http://dx.doi.org/10.1098/rspa.2015.0229

Received: 8 April 2015
Accepted: 30 June 2015

Subject Areas:
mechanics, nanotechnology

Keywords:
binding energy, carbon nanotubes, beam model

Author for correspondence:
Junhua Zhao
e-mail: junhua.zhao@jiangnan.edu.cn

Binding energy and mechanical stability of two parallel and crossing carbon nanotubes

Junhua Zhao[1], Yue Jia[2], Ning Wei[3] and Timon Rabczuk[2]

[1]Jiangsu Key Laboratory of Advanced Food Manufacturing Equipment and Technology, Jiangnan University, Wuxi 214122, People's Republic of China
[2]Institute of Structural Mechanics, Bauhaus-University Weimar, 99423 Weimar, Germany
[3]College of Water Resources and Architectural Engineering, Northwest A&F University, Yangling 712100, People's Republic of China

The binding energy between two parallel (and two crossing) single-walled (and multi-walled) carbon nanotubes (CNTs) is obtained by continuum modelling of the van der Waals interaction between them. The dependence of the binding energy on their diameters, number of walls and crossing angles is systematically analysed. The critical length for the mechanical stability and adhesion of the CNTs is determined by the function of E_iI_i, h and γ, where E_iI_i, h and γ are the CNTs bending stiffness, distance and binding energy between them, respectively. Checking against full atom molecular dynamics calculations show that the continuum solution has high accuracy. The established analytical solutions should be of great help for designing nanoelectromechanical devices.

1. Introduction

The unique mechanical, electrical, thermal and optical properties of carbon nanotubes (CNTs) enable them highly potential and ideal candidates for multifarious applications [1–3]. CNT exists in several structures forms such as single-walled CNTs (SWCNTs), multi-walled CNTs (MWCNTs), bundles and networks [4,5]. The mechanical properties of SWCNTs and MWCNTs

THE ROYAL SOCIETY PUBLISHING

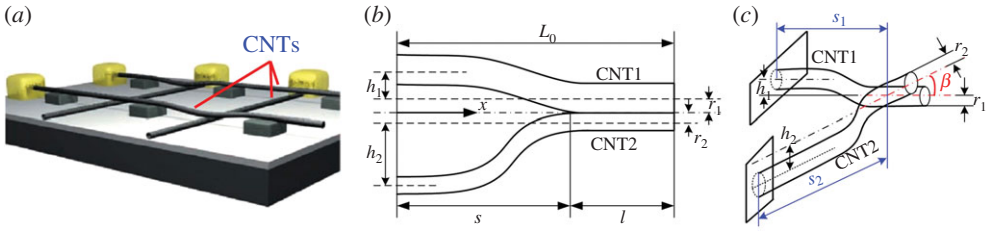

Figure 1. Schematic diagrams showing the fabrication process of CNT electronic devices and the geometry of two parallel and two crossing CNTs under adherent conditions. (*a*) The fabrication process of CNT electronic devices [18], (*b*) two parallel CNTs and (*c*) two crossing CNTs. (Online version in colour.)

have been extensively studied in previous work [6–9]. Recently, the CNT networks have been taken as a potential energy-saving material [10], while the CNT bundles have potential applications in nanocomposites materials. In the synthesis of CNT bundles and networks, their formation is a challenge for understanding how to measure and predict the properties of such large systems [4,11]. At the nanoscale, the weak van der Waals (vdW) interactions govern the structural organization and the mechanical properties of CNT bundles and networks [12–15]. Therefore, a clear understanding of the vdW interactions in these systems is crucial for their potential applications in nanoelectromechanical systems and electronic devices. The self-folding of SWCNTs, MWCNTs and multi-layer graphene sheets has been investigated and the bundle pattern formation has also been studied in previous work [14–16]. However, all their binding energies were from full atom molecular dynamics (MD) simulation or experimental results. Girifalco *et al.* [17] obtained the cohesive energy between two parallel and same radii SWCNTs using atomistic models. In recent years, a suspended SWCNT crossbar array for both I/O and switchable, bistable device elements with well-defined OFF and ON states has been exploited by Rueckes *et al.* [18]. The crossbar consists of a set of parallel SWCNTs on a substrate and a set of perpendicular SWCNTs that are suspended on a periodic array of supports (figure 1*b*). It was found that the mechanical stability of the structures is determined by the vdW interactions between the two SWCNTs [18]. Because the vdW interactions between the two SWCNTs dominate the working reliability of the bistable device, the key issue of the binding energy and mechanical stability of two parallel and crossing CNTs has to be solved in order to clearly understand the working mechanism of the bistable device.

In this paper, the binding energy between two parallel (and two crossing) SWCNTs (and MWCNTs) is obtained from a continuum model based on the Lennard-Jones (LJ) potential. The analytical expressions are validated by comparing with our full atom MD simulations. Since the critical length for the mechanical stability and adhesion of the two CNTs dominate the working reliability of a bistable device, it is significant to derive their analytical solutions.

2. Analytical model of binding energy and mechanical stability

Figure 1 shows the two parallel CNTs (*b*) and two crossing CNTs (*c*) under adherent conditions, in which the two CNT radii can be different. To determine the critical and stable lengths where the two CNTs do not make contact, an analytical model is presented in this paper and the corresponding geometry of the problem is plotted in figure 1. Some assumptions are proposed to simplify the problem: (i) the two CNTs are taken as two cantilever beams and the shear deformation are ignored. (ii) The closest distance between the adherent components of the two CNTs is taken as zero (or a constant d which does not influence the results). (iii) The radii of CNTs and the displacement between the two CNTs are both far less than the length L_0, that is to say, L_0 is approximately equal to $s + l$ under adherent conditions.

As shown in figure 1*b*, the total energy is composed of elastic energy and adhesion energy.

$$U_T = U_{\mathrm{CNT1}} + U_{\mathrm{CNT2}} - \gamma(L_0 - s), \tag{2.1}$$

where U_{CNT1}, U_{CNT2} and γ are elastic energy of CNT1 and CNT2 as well as binding energy per unit length, respectively.

Based on the present boundary condition, the total energy of equation (2.1) can be expressed as

$$U_T = \frac{6(E_1 I_1 h_1^2 + E_2 I_2 h_2^2)}{s^3} - \gamma(L_0 - s), \tag{2.2}$$

where E_1 and E_2 are Young's moduli of CNT1 and CNT2, and I_1 and I_2 are the moment of inertia of CNT1 and CNT2, respectively.

For an SWCNT, the bending stiffness of the beam is [19]

$$EI = \frac{\pi E}{4}[r^4 - (r-t)^4], \tag{2.3}$$

where r and t (0.34 nm is chosen here) are the radius and the thickness of the SWCNT, respectively.

For an MWCNT, the bending stiffness of the beam is [20,21]

$$(EI)_{\mathrm{MW}} = (EI)_{\mathrm{inner}} m \left[1 + \frac{3(m-1)}{2}\frac{\sigma}{r_{\mathrm{inner}}} + \frac{(m-1)(2m-1)}{2}\frac{\sigma^2}{r_{\mathrm{inner}}^2} + \frac{m(m-1)^2}{4}\frac{\sigma^3}{r_{\mathrm{inner}}^3}\right], \tag{2.4}$$

where $(EI)_{\mathrm{inner}}$ and r_{inner} are the bending stiffness and radius of the innermost wall, respectively, m is the number of walls, and $\sigma = 0.34$ nm is the interwall spacing.

In view of the equilibrium of system, the total energy should be a minimum value. The critical value of s can be obtained by $\mathrm{d}U_T/\mathrm{d}s = 0$, that is given

$$L_0^{\mathrm{critical}} = \left(\frac{18(E_1 I_1 h_1^2 + E_2 I_2 h_2^2)}{\gamma}\right)^{1/4}. \tag{2.5}$$

The critical length L_0^{critical} represents a critical value, in which the two parallel cantilever CNTs stick together when the lengths of the two CNTs are both higher than L_0^{critical} for a given CNT diameter and a distance h.

If $E_1 = E_2 = E$ and $I_1 = I_2 = I$ (that is, CNT1 = CNT2), then $h_1 = h_2 = h$ and equation (2.5) can be written as

$$L_0^{\mathrm{critical}} = \left(\frac{36\mathrm{EI}h^2}{\gamma}\right)^{1/4}. \tag{2.6}$$

For two crossing CNTs, the stability length of the CNTs can be obtained from

$$U_T = U_{\mathrm{CNT1}} + U_{\mathrm{CNT2}} - \gamma_{\mathrm{crossing}} \geq 0, \tag{2.7}$$

where $\gamma_{\mathrm{crossing}}$ is the absolute minimum of the cohesive energy between two crossing CNTs at the equilibrium distance. If we assume the s_1 and s_2 of the two crossing CNTs are both the same, we can obtain the stability length from equations (2.2) and (2.7),

$$L_0^{\mathrm{stability}} = \left(\frac{6(E_1 I_1 h_1^2 + E_2 I_2 h_2^2)}{\gamma_{\mathrm{crossing}}}\right)^{1/3}. \tag{2.8}$$

The stable length $L_0^{\mathrm{stability}}$ represents another critical value, in which the two crossing cantilever CNTs stick together when the lengths of the two CNTs are both higher than $L_0^{\mathrm{stability}}$ for a given CNT diameter and a distance h.

If $E_1 = E_2 = E$ and $I_1 = I_2 = I$ (i.e. CNT1 = CNT2), then $h_1 = h_2 = h$ and equation (2.8) can be written as

$$L_0^{\text{stability}} = \left(\frac{12EIh^2}{\gamma_{\text{crossing}}}\right)^{1/3}. \tag{2.9}$$

From equations (2.5) and (2.9), how to determine γ and γ_{crossing} between two parallel CNTs and two crossing CNTs is a crucial issue in this work.

For two parallel SWCNTs, the cohesive energy per unit length has been obtained [22] as

$$\varphi_{\text{circle}} = \pi \in \sigma^6 \rho^2 r_1 r_2 \left(\frac{63}{8}\sigma^6 \int_0^{\pi} \frac{F_5[2\sqrt{a_0 r_1}/(r_1 + a_0)]}{(r_1 + a_0)^{11}} \mathrm{d}\theta_2 - 12 \int_0^{\pi} \frac{F_2\left[2\sqrt{a_0 r_1}/(r_1 + a_0)\right]}{(r_1 + a_0)^5} \mathrm{d}\theta_2\right), \tag{2.10}$$

where $\in$ and σ are, respectively, the depth and the equilibrium distance of the 6–12 LJ potential between two carbon atoms ($\in = 2.8437$ mev and $\sigma = 3.4$ Å are adopted from the literature) [6,7], and ρ is the area density CNTs, and r_1 and r_2 are the radii of the two CNTs, and $a_0 = \sqrt{(r_1 + r_2 + h)^2 + r_2^2 + 2(r_1 + r_2 + h) r_2 \cos\theta_2}$, and F_5 and F_2 can be found in our previous work [22]. The binding energy γ per unit length is the absolute minimum of ϕ_{circle} at equilibrium distance between the two SWCNTs.

For two crossing SWCNTs, the total cohesive energy has been obtained [22] as

$$\phi_{\text{total}} = 4\rho^2 r_1 r_2 \in \sigma^6 \frac{1}{\sin\beta}\left(\frac{63\pi}{128}\sigma^6 \int_0^{\pi} \frac{A_0 B_0 S_0}{S_d} \mathrm{d}\theta_2 - \frac{3\pi}{4} \int_0^{\pi} \frac{A_1 B_1 T_1}{T_d} \mathrm{d}\theta_2\right), \quad \left(0 < \beta \le \frac{\pi}{2}\right), \tag{2.11}$$

where

$$\begin{aligned} S_0 =& 362880 a_0^9 \cos^9\theta_0 + 6531840 a_0^7 \cos^7\theta_0 r_1^2 + 17146080 a_0^5 \cos^5\theta_0 r_1^4 \\ &+ 9525600 a_0^3 \cos^3\theta_0 r_1^6 + 893025 a_0 \cos\theta_0 r_1^8, \\ A_0 =& -1/128(98 + (36/5) - (2/63)), B_0 = -2\pi/9!, S_d = [(r_1 + r_2 + h + r_2\cos\theta_2)^2 - r_1^2]^{19/2}, \\ T_1 =& 6a_0^3 \cos^3\theta_0 + 9a_0 \cos\theta_0 r_1^2, A_1 = -4/3, B_1 = -2\pi/3!, \\ T_d =& [(r_1 + r_2 + h + r_2\cos\theta_2)^2 - r_1^2]^{7/2}, \theta_0 = \arccos((r_1 + r_2 + h)^2 + a_0^2 - r_2^2/2(r_1 + r_2 + h)a_0), \end{aligned}$$

and β is the crossing angle between the two centre axes of the two crossing CNTs [22]. The binding energy γ_{crossing} is the absolute minimum of ϕ_{total} at equilibrium distance between the two SWCNTs.

Figure 2*a* shows the binding energy distribution with CNT radius between two parallel SWCNTs and two crossing SWCNTs using equations (2.10) and (2.11) and full atom MD simulations, in which the MD simulation is performed using LAMMPS [23] with the AIREBO potential and periodic boundary conditions are applied along the centre axis of the CNTs (the LJ cut-off radius is 60 Å, which is enough distance to get accurate results). The analytical results are in good agreement with those from our full atom MD simulations. Figure 2*b* shows the analytical binding energy between two different parallel SWCNTs and two different crossing SWCNTs.

Figure 3 shows an SWCNT parallel to an MWCNT. We assume that the distance between any two neighbour CNTs in the MWCNT is 3.4 Å.

Based on equations (2.10) and (2.11), the cohesive energy between the ith CNT in the MWCNT and an SWCNT should be easily obtained as

$$\phi_{i0} = \pi \in \sigma^6 \rho^2 r_0 r_i \left(\frac{63}{8}\sigma^6 \int_0^{\pi} \frac{F_5[2\sqrt{a_0 r_0}/(r_0 + a_0)]}{(r_0 + a_0)^{11}} \mathrm{d}\theta_2 - 12 \int_0^{\pi} \frac{F_2[2\sqrt{a_0 r_0}/(r_0 + a_0)]}{(r_0 + a_0)^5} \mathrm{d}\theta_2\right), \tag{2.12}$$

where $a_0 = \sqrt{[r_0 + r_i + (3.4(i-1) + h_1)]^2 + r_i^2 + 2(r_0 + r_i + (3.4(i-1) + h_1))r_i\cos\theta_2}$, h_1 is the distance between the SWCNT and the outmost CNT in the MWCNT (figure 3).

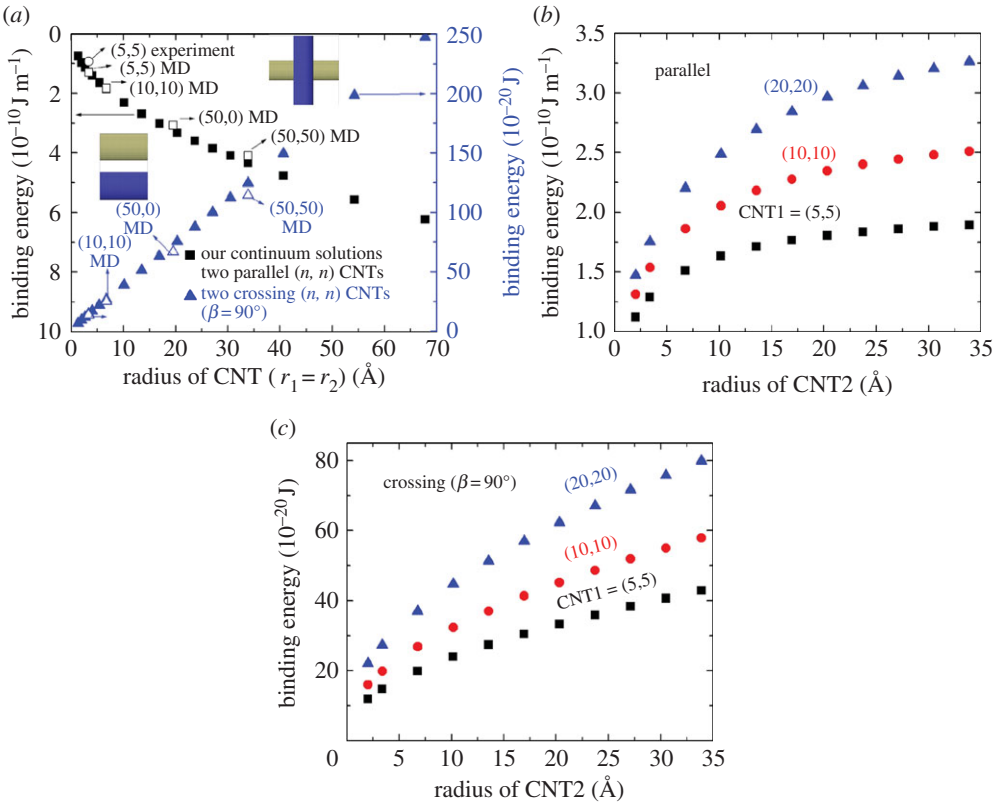

Figure 2. The binding energy distribution with CNT radius between two parallel SWCNTs and two crossing SWCNTs. (*a*) two same radii SWCNTs, (*b*) two parallel, different radii SWCNTs and (*c*) two crossing, different radii SWCNTs. (Online version in colour.)

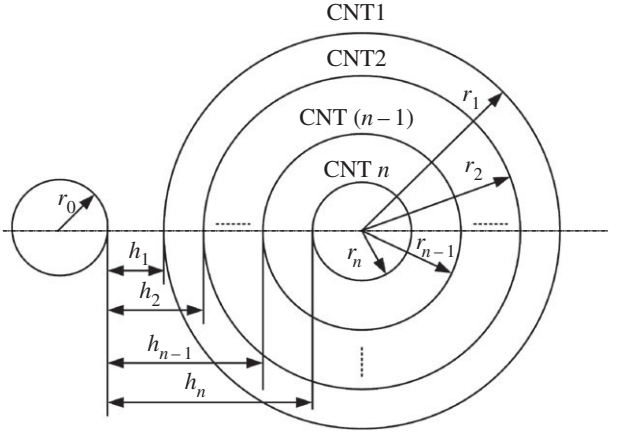

Figure 3. A schematic diagram of an SWCNT parallel to an MWCNT.

The total cohesive energy from equation (2.12) should be given as

$$\phi_{\mathrm{MW-SW}} = \pi \in \sigma^6 \rho^2 r_0 \sum_{1\le i\le n} r_i \times \left(\frac{63}{8}\sigma^6 \int_0^{\pi} \frac{F_5[(2\sqrt{a_0 r_0}/(r_0+a_0))]}{(r_0+a_0)^{11}}\,\mathrm{d}\theta_2 - 12\int_0^{\pi} \frac{F_2[2\sqrt{a_0 r_0}/(r_0+a_0)]}{(r_0+a_0)^5}\,\mathrm{d}\theta_2 \right), \quad (2.13)$$

where a_0 is the same as that in equation (2.11).

Similarly, the total energy between two parallel MWCNTs can be obtained

$$\phi_{\mathrm{MW-MWparallel}} = \pi \in \sigma^6 \rho^2 \sum_{1\le j\le m} \sum_{1\le i\le n} r_i r_j \times \left(\frac{63}{8}\sigma^6 \int_0^{\pi} \frac{F_5[(2\sqrt{a_0 r_j}/(r_j + a_0))]}{(r_j + a_0)^{11}}\, \mathrm{d}\theta_2 - 12 \int_0^{\pi} \frac{F_2[2\sqrt{a_0 r_j}/(r_j + a_0)]}{(r_j + a_0)^5}\, \mathrm{d}\theta_2 \right), \tag{2.14}$$

where $a_0 = \sqrt{[r_j + r_i + (3.4(i + j - 2) + 2h_1)]^2 + r_i^2 + 2(r_j + r_i + (3.4(i + j - 2) + 2h_1))r_i \cos\theta_2}$, m is the number of the walls in the other MWCNT, h_1 is the distance between the outmost CNT in one MWCNT and the outmost CNT in the other MWCNT.

Similarly, the total energy between two crossing MWCNTs can be obtained

$$\phi_{\mathrm{MW-MWcross}} = 4\rho^2 \in \sigma^6 \frac{1}{\sin\beta} \sum_{1\le j\le m} \sum_{1\le i\le n} r_i r_j \left(\frac{63\pi}{128}\sigma^6 \int_0^{\pi} \frac{A_0 B_0 S_0}{S_d}\, \mathrm{d}\theta_2 - \frac{3\pi}{4} \int_0^{\pi} \frac{A_1 B_1 T_1}{T_d}\, \mathrm{d}\theta_2 \right), \tag{2.15}$$

where

$$\theta_0 = \arccos \frac{(r_i + r_j + (3.4(i + j - 2) + 2h_1))^2 + a_0^2 - r_j^2}{2(r_i + r_j + (3.4(i + j - 2) + 2h_1))a_0},$$

$$S_0 = 362880a_0^9 \cos^9\theta_0 + 6531840a_0^7 \cos^7\theta_0 r_i^2 + 17146080a_0^5 \cos^5\theta_0 r_i^4 + 9525600a_0^3 \cos^3\theta_0 r_i^6 + 893025a_0 \cos\theta_0 r_i^8,$$

$$S_d = [(r_i + r_j + (3.4(i + j - 2) + 2h_1) + r_j \cos\theta_2)^2 - r_i^2]^{19/2}, T_1 = 6a_0^3 \cos^3\theta_0 + 9a_0 \cos\theta_0 r_i^2,$$

$$T_d = \left[(r_i + r_j + (3.4(i + j - 2) + 2h_1) + r_j \cos\theta_2)^2 - r_i^2\right]^{7/2}, a_0$$

is the same as that in equation (2.14), and the other parameters are the same as those in equation (2.11).

Figure 4 shows the binding energy between two parallel MWCNTs and two crossing MWCNTs from our analytical model, in which the innermost CNT is the (5,5) CNT. The binding energy nonlinearly increases with increasing number of walls.

3. Molecular dynamics simulations

Figure 5 shows the critical length and stable length for two parallel SWCNTs and two crossing SWCNTs based on our analytical results and full atom MD simulations. To obtain the bending stiffness from the MD simulations, the initial atomic structure of a (5,5) CNT is optimized by the MD method, such that the total potential energy is minimized and forces between atoms are zero before the bending deformation. To apply bending deformation, rigid body translation is applied to the atoms in both end layers of the CNT, such that both end sections remain circular and are kept perpendicular to the deformed axis in each displacement increment; the length of the deformed tube axis remains unchanged and its curvature is essentially uniform throughout deformation. The displacement-controlled loading is widely used in literature to simulate the pure bending deformation of SWCNTs in MD [24]. The bending stiffness $EI = 3.95 \times 10^{-26}$ J m of the (5,5) CNT is obtained by our MD results by LAMMPS software with AIREBO potential (figure 5*a*), which is close to the available value 3.84×10^{-26} J m from previous work [25]. U_{bending} is the bending energy per unit length and κ is the $1/r$, in which r is the curvature radius and the (5,5) CNT length is equal to 11.6 nm in figure 5*a* [22] and the detailed MD process is the same as previous work [24]. To obtain the critical length of figure 5*b* for two parallel SWCNTs by full atom MD simulations, we keep the initial distance around 30 Å between two parallel SWCNTs, where vdW interactions are considerably weaker and can be ignored. After the energy minimization, the

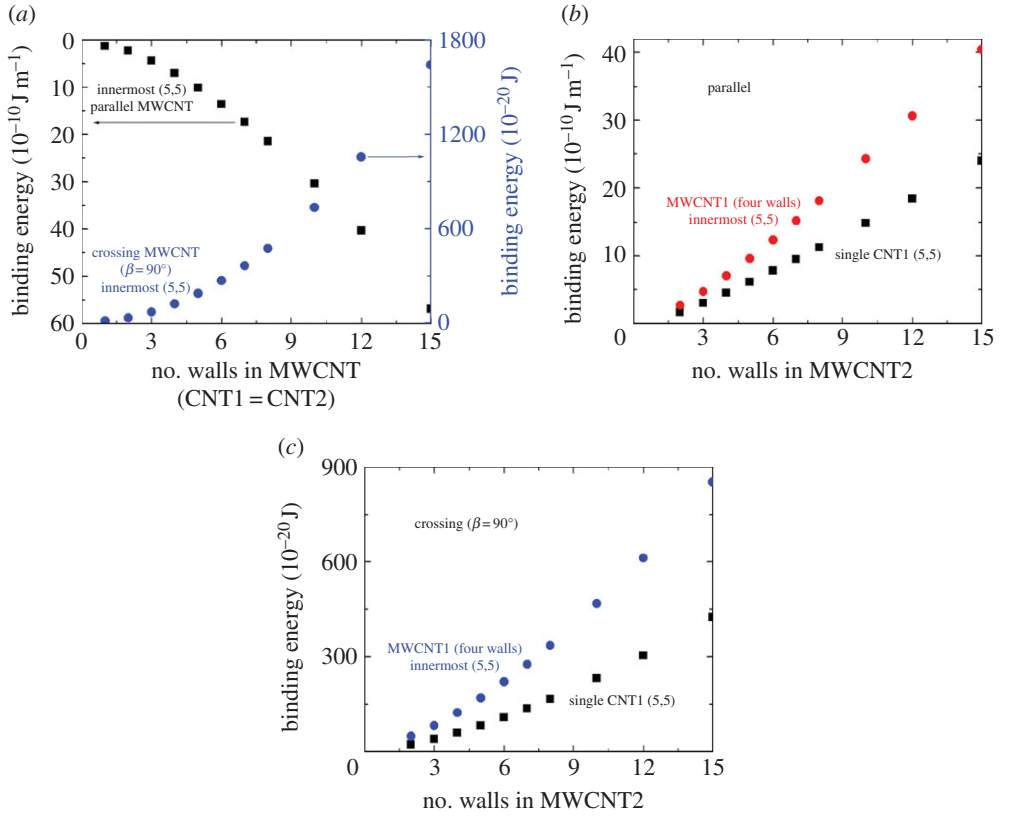

Figure 4. The binding energy distribution with CNT radius between two parallel MWCNTs and two crossing MWCNTs. (*a*) two same radii MWCNTs, (*b*) two parallel, different radii MWCNTs and (*c*) two crossing, different radii MWCNTs. (Online version in colour.)

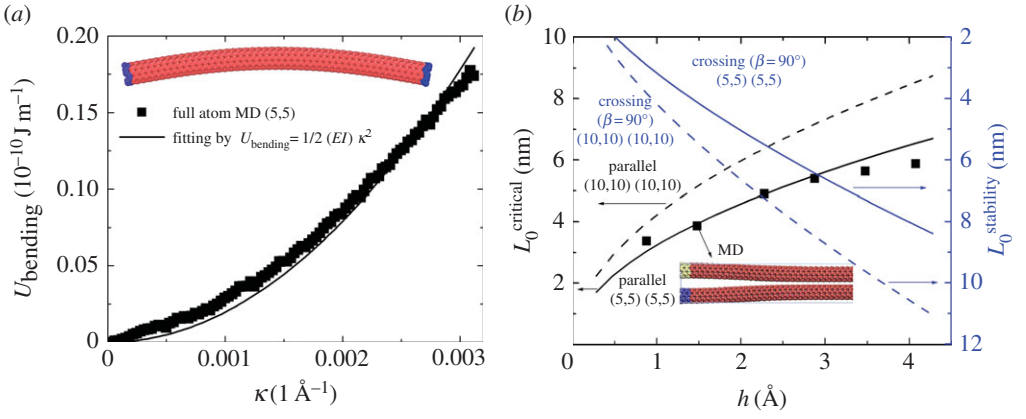

Figure 5. (*a*) The bending stiffness of a (5,5) CNT by full atom MD simulation, and (*b*) the critical length and stable length for two parallel SWCNTs and two crossing SWCNTs based on our analytical results and full atom MD simulations. (Online version in colour.)

left ends of the two parallel SWCNTs (see the yellow and blue ends on the SWCNTs in the inset of figure 5*b*) are always fixed, while all right ends of the SWCNTs are free. The present simulation is at 0 K and the upper SWCNT gets gradually closer to the lower one with an increment of 0.1 Å per time step based on the deformation-control method. Afterwards, the optimized structure is taken as the initial geometry for the next calculations. The right ends of the two SWCNTs will

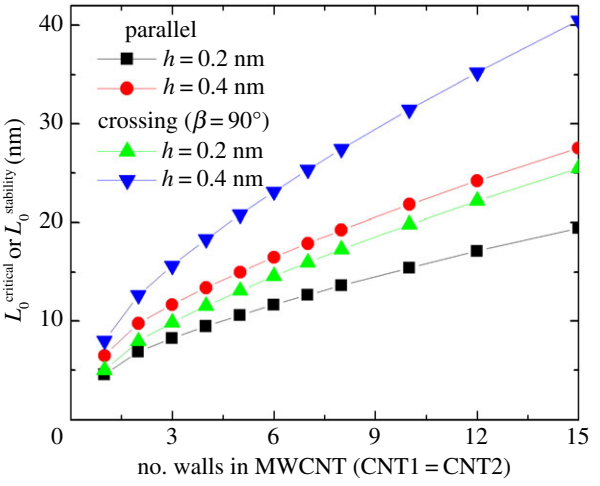

Figure 6. The critical length and stable length with number of walls for two parallel MWCNTs and two crossing MWCNTs based on our analytical results. (Online version in colour.)

stick together when the distance between the two SWCNTs is close enough. For a given close distance between two CNTs, the right ends of the two cantilever CNTs will stick together and the length of the stuck part increases with decreasing distance. The present analytical results are in good agreement with those from MD simulations for two parallel (5,5) CNTs in figure 5*b*.

Figure 6 shows the critical length and stable length for two parallel MWCNTs and two crossing MWCNTs based on our analytical results. For a given distance (the distance between the two outmost CNTs in the two MWCNTs (figure 1)), both the critical length and the stable length nonlinearly increase with increasing number of walls.

4. Conclusion

In summary, the analytical expressions (such as equations (2.13)–(2.15)) of the binding energy between two parallel (and two crossing) single-walled (and multi-walled) CNTs are obtained by continuum modelling of the vdW interactions between them. The dependence of the binding energy on their diameters, number of walls and crossing angles is systematically analysed. The critical length for the mechanical stability and adhesion (such as equations (2.5), (2.6), (2.8) and (2.9)) of the CNTs has been determined by the function of E_iI_i, h and γ, where E_iI_i, h and γ are the CNT bending stiffness, distance and binding energy between them, respectively. Checking against full atom MD calculations show that the continuum solution has high accuracy. The established analytical solutions should be of great help for designing nanoelectromechanical devices.

Authors' contributions. J.Z. performed all the calculations, interpreted the results and wrote the manuscript. Y.J., N.W. and T.R. helped to interpret the results and edited the manuscript. All authors gave final approval for publication.

Competing interests. We declare we have no competing interests.

Funding. Financial support was provided by the National Natural Science Foundation of China (grant no.11302084), the Fundamental Research Funds for the Central Universities (grant no. JUSRP11529), Open Fund of Key Laboratory for Intelligent Nano Materials and Devices of the Ministry of Education (NUAA) (grant no. INMD-2015M01) is kindly acknowledged.

Acknowledgements. We gratefully acknowledge support from the 'Thousand Youth Talents Plan'.

References

1. Iijima S. 1991 Helical microtubules of graphitic carbon. *Nature* **354**, 56–58. (doi:10.1038/354056a0)

2. Baughman RH, Zakhidov AA, de Heer WA. 2002 Carbon nanotubes-the route toward applications. *Science* **297**, 787–792. (doi:10.1126/science.1060928)
3. Modi A, Koratkar N, Lass E, Wei BQ, Ajayan PM. 2003 Miniaturized gas ionization snsors using carbon nanotubes. *Nature* **424**, 171–174. (doi:10.1038/nature01777)
4. Ajayan PM, Banhart F. 2002 Strong bundles. *Nat. Mater.* **3**, 135–136. (doi:10.1038/nmat1078)
5. Bronikowski M. 2006 CVD growth of carbon nanotube bundle arrays. *Carbon* **44**, 2822–2832. (doi:10.1016/j.carbon.2006.03.022)
6. Yakobson BI, Brabec CJ, Bernholc J. 1996 Nanomechanics of carbon tubes: instability beyond linear response. *Phys. Rev. Lett.* **76**, 2511–2514. (doi:10.1103/PhysRevLett.76.2511)
7. Chang T, Gao H. 2003 Size-dependent elastic properties of a single-walled carbon nanotube via a molecular mechanics model. *J. Mech. Phys. Solids* **51**, 1059–1074. (doi:10.1016/S0022-5096(03)00006-1)
8. Li CY, Chou TW. 2003 A structural mechanics approach for the analysis of carbon nanotubes. *Int. J. Solids Struct.* **40**, 2487–2499. (doi:10.1016/S0020-7683(03)00056-8)
9. Li H, Guo W. 2008 Transversely isotropic elastic properties of single-walled carbon nanotubes by a rectangular beam model for the C-C bonds. *J. Appl. Phys.* **103**, 103501. (doi:10.1063/1.2930999)
10. Xie B, Liu Y, Ding Y, Zheng Q, Xu Z. 2011 Mechanics of carbon nanotube networks: microstructural evolution and optimal design. *Soft Matter* **7**, 10 039–10 047. (doi:10.1039/c1sm06034a)
11. Kis A, Csanyi G, Salvetat JP, Lee TN, Couteau E, Kulik AJ, Benoit W, Brugger J, Forro L. 2004 Reinforcement of single-walled carbon nanotube bundles by intertube bridging. *Nat. Mater.* **3**, 153–157. (doi:10.1038/nmat1076)
12. Ru CQ. 2000 Effect of van der Waals forces on axial buckling of a double-walled carbon nanotube. *J. Appl. Phys.* **87**, 7227. (doi:10.1063/1.372973)
13. Ru CQ. 2001 Axially compressed buckling of a doublewalled carbon nanotube embedded in an elastic medium. *J. Mech. Phys. Solids* **49**, 1265–1279. (doi:10.1016/S0022-5096(00)00079-X)
14. Huang W Liu Y Hwang B Zuo KC Buehler JM andGao MJ Zhou H. 2007 Self-folding of single- and multiwall carbon nanotubes. *Appl. Phys. Lett.* **90**, 073107. (doi:10.1063/1.2535874)
15. Cranford S, Yao H, Ortiz C, Buehler MJ. 2010 A single degree of freedom 'lollipop' model for carbon nanotube bundle formation. *J. Mech. Phys. Solids* **58**, 409–427. (doi:10.1016/j.jmps.2009.11.002)
16. Cranford S, Sen D, Buehler MJ. 2009 Meso-origami: folding multilayer graphene sheets. *Appl. Phys. Lett.* **95**, 123121. (doi:10.1063/1.3223783)
17. Girifalco LA, Hodak M, Lee R. 2000 Carbon nanotubes, buckyballs, ropes, and a universal graphitic potential. *Phys. Rev. B* **62**, 13104. (doi:10.1103/PhysRevB.62.13104)
18. Rueckes T, Kim K, Joselevich E, Tseng GY, Cheung CL, Lieber CM. 2000 Carbon nanotube-based nonvolatile random access memory for molecular computing. *Science* **289**, 94–97. (doi:10.1126/science.289.5476.94)
19. Timoshenko S, Maccullough GH 1935 *Elements of strength of materials*. New York, NY: Van Nostrand.
20. Pantano A, Boyce MC, Parks DM. 2003 Nonlinear structural mechanics based modeling of carbon nanotube deformation. *Phys. Rev. Lett.* **91**, 145504. (doi:10.1103/PhysRevLett.91.145504)
21. Pantano A, Parks DM, Boyce MC. 2004 Mechanics of deformation of single and multi-wall carbon nanotubes. *J. Mech. Phys. Solids* **52**, 789–821. (doi:10.1016/j.jmps.2003.08.004)
22. Zhao J, Jiang JW, Jia Y, Guo W, Rabczuk T. 2013 A theoretical analysis of cohesive energy between carbon nanotubes, graphene and substrates. *Carbon* **57**, 108–119. (doi:10.1016/j.carbon.2013.01.041)
23. Plimpton S. 1995 Fast parallel algorithms for short-range molecular dynamics. *J. Comput. Phys.* **117**, 1–19. (doi:10.1006/jcph.1995.1039)
24. Cao G, Chen X. 2006 Buckling of single-walled carbon nanotubes upon bending: Molecular dynamics simulations and finite element method. *Phys. Rev. B* **73**, 155435. (doi:10.1103/PhysRevB.73.155435)
25. Chen B, Gao M, Zuo JM, Qu S, Liu B, Huang Y. 2003 Binding energy of parallel carbon nanotubes. *Appl. Phys. Lett.* **83**, 3570–3571. (doi:10.1063/1.1623013)